

University of Groningen

Photosynthetic Quantum Yield Dynamics

Hogewoning, Sander W.; Wientjes, Emilie; Douwstra, Peter; Trouwborst, Govert; van Ieperen, Wim; Croce, Roberta; Harbinson, Jeremy

Published in:
 Plant Cell

DOI:
[10.1105/tpc.112.097972](https://doi.org/10.1105/tpc.112.097972)

IMPORTANT NOTE: You are advised to consult the publisher's version (publisher's PDF) if you wish to cite from it. Please check the document version below.

Document Version
 Publisher's PDF, also known as Version of record

Publication date:
 2012

[Link to publication in University of Groningen/UMCG research database](#)

Citation for published version (APA):

Hogewoning, S. W., Wientjes, E., Douwstra, P., Trouwborst, G., van Ieperen, W., Croce, R., & Harbinson, J. (2012). Photosynthetic Quantum Yield Dynamics: From Photosystems to Leaves. *Plant Cell*, 24(5), 1921-1935. <https://doi.org/10.1105/tpc.112.097972>

Copyright

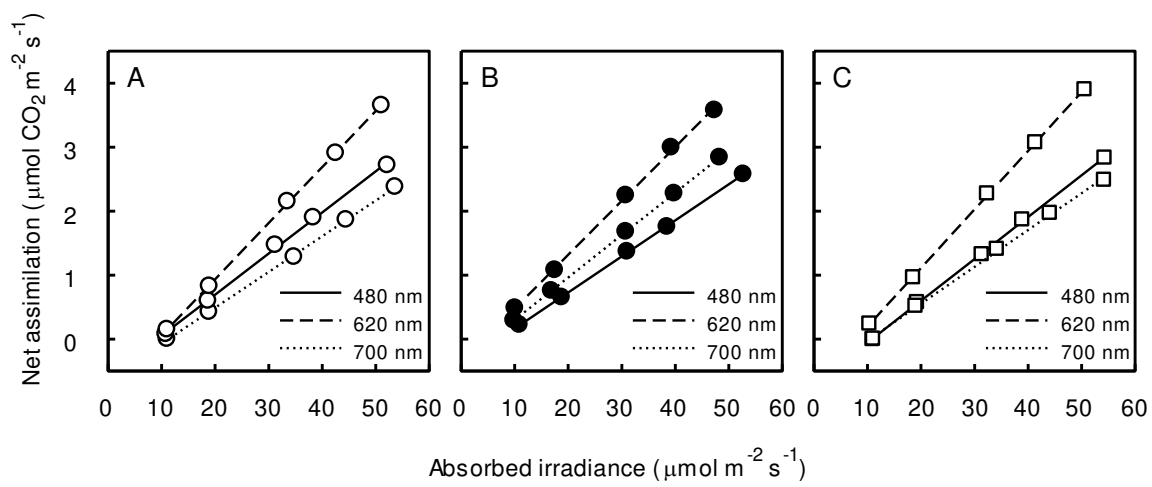
Other than for strictly personal use, it is not permitted to download or to forward/distribute the text or part of it without the consent of the author(s) and/or copyright holder(s), unless the work is under an open content license (like Creative Commons).

The publication may also be distributed here under the terms of Article 25fa of the Dutch Copyright Act, indicated by the "Taverne" license. More information can be found on the University of Groningen website: <https://www.rug.nl/library/open-access/self-archiving-pure/taverne-amendment>.

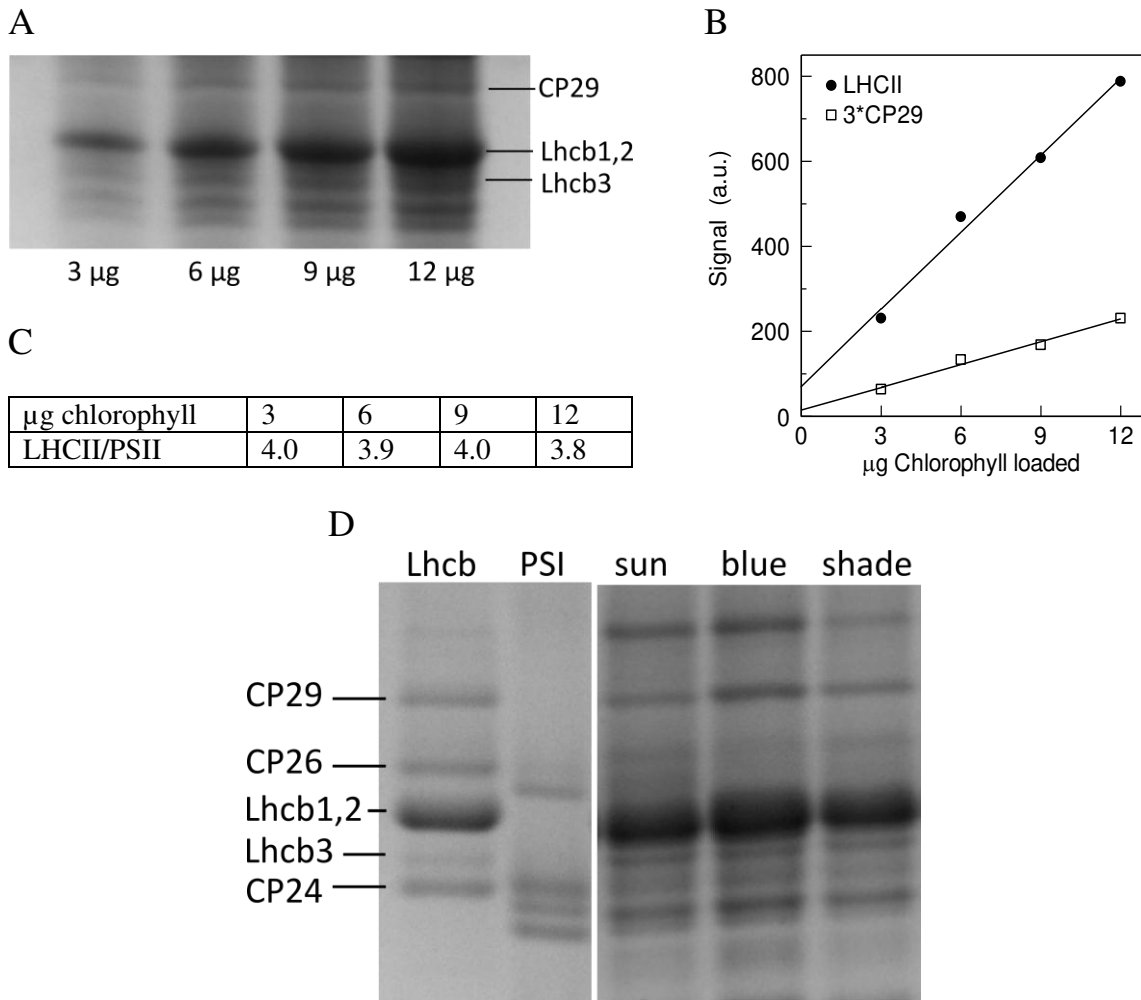
Take-down policy

If you believe that this document breaches copyright please contact us providing details, and we will remove access to the work immediately and investigate your claim.

Downloaded from the University of Groningen/UMCG research database (Pure): <http://www.rug.nl/research/portal>. For technical reasons the number of authors shown on this cover page is limited to 10 maximum.



Supplemental Figure 1. Typical responses of net assimilation to irradiance within the light-limited range for leaves grown under a sunlight spectrum **(A)**, a shadelight spectrum **(B)** and blue light **(C)**. The slope of each curve expresses the quantum yield for CO₂ fixation for the corresponding wavelength.



Supplemental Figure 2. Analysis of LHCII content in thylakoids of leaves grown under a sunlight spectrum, a shadelight spectrum, and blue light by SDS PAGE. **(A)** Example of SDS-PAGE for thylakoids (sunlight) loaded at 4 different concentrations. **(B)** Linearity verification of Coomassie bound to CP29 and LHCII. Values of integrated optical density of the bands are plotted against the quantity of material loaded. **(C)** LHCII trimers/PSII based on the four different concentrations of thylakoids (example for shadelight spectrum grown leaves). **(D)** Analysis of LHCII content. SDS-PAGE was followed by Coomassie staining, and densitometric analysis of the polypeptide was used to quantify LHCII (Lhcb1-3) levels relative to CP29 (Lhcb4). Preparations containing the monomeric Lhcb antenna and PSI complexes were used as references. For the thylakoids of the leaves 12 µg of chlorophylls were loaded. The Lhcb region of the gel is shown. Note that the PSI proteins do not overlap with CP29 or Lhcb1-3.

The PSI/PSII ratio (Table 1 main text) was calculated from the Chl a:b ratio of the membranes using the Chl content values of PSI-LHCI, PSII core, LHCII trimer and minor Lhcb (see Table 2 main text) and the LHCII:PSII core ratio obtained for each sample from the analysis of the SDS page gel. The Chl a:b ratio is given by:

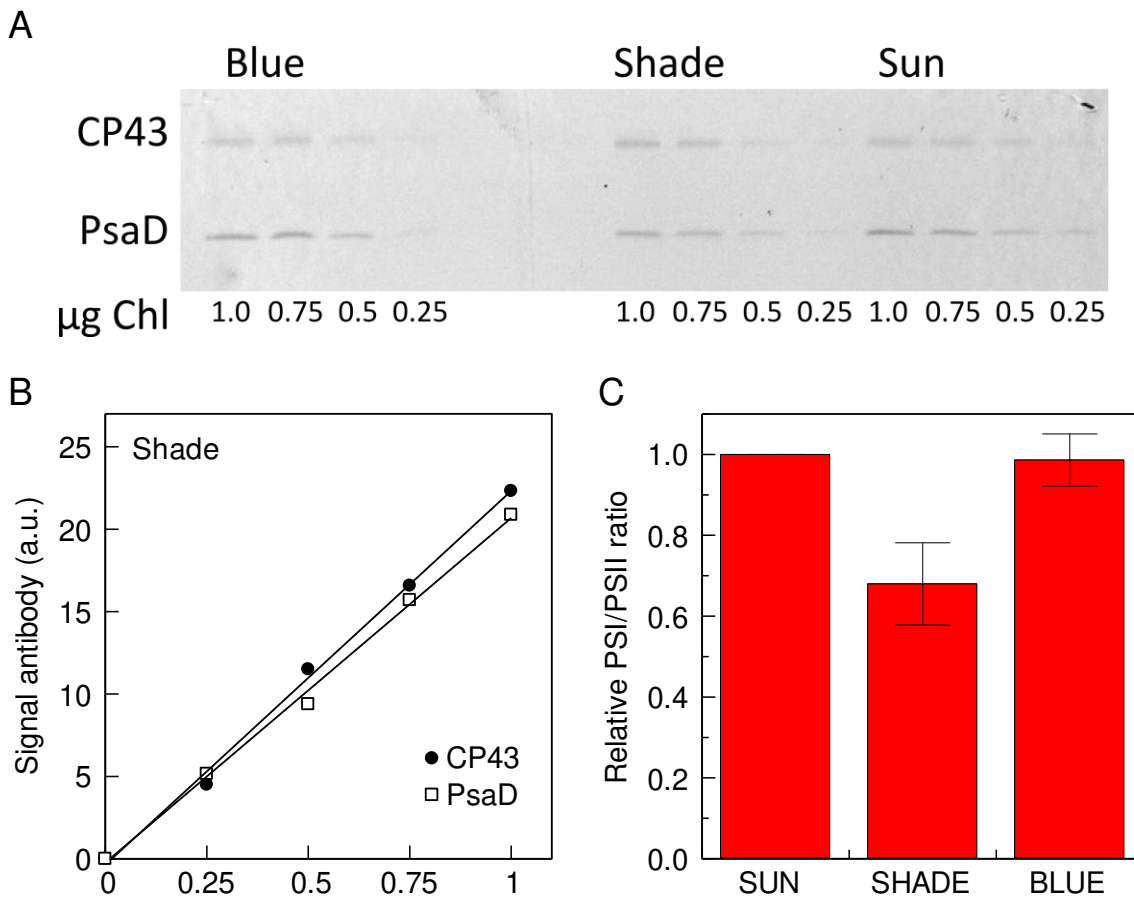
$$\frac{Chla}{Chlb} = \frac{150.3 * PSI + 37 * PSII + 23.7 * n_{LHCII} * PSII + 17 * PSII}{17.7 * PSI + 18.3 * n_{LHCII} * PSII + 10 * PSII}$$

PSI and PSII are on RC (reaction centre) basis and n_{LHCII} represents the number of LHCII trimers per PSII RC. Taking PSII as 1, this simplifies to:

$$\frac{Chla}{Chlb} = \frac{54 + 150.3 * PSI + 23.7 * n_{LHCII}}{17.7 * PSI + 18.3 * n_{LHCII} + 10}$$

From which can be derived that PSI/PSII, as a function of the Chl a:b ratio and the number of LHCII trimers per PSII RC, is calculated as:

$$\frac{PSI}{PSII} = \frac{54 + n_{LHCII} * 23.7 - (18.3 * n_{LHCII} + 10) * \frac{Chla}{Chlb}}{17.7 * \frac{Chla}{Chlb} - 150.3}$$

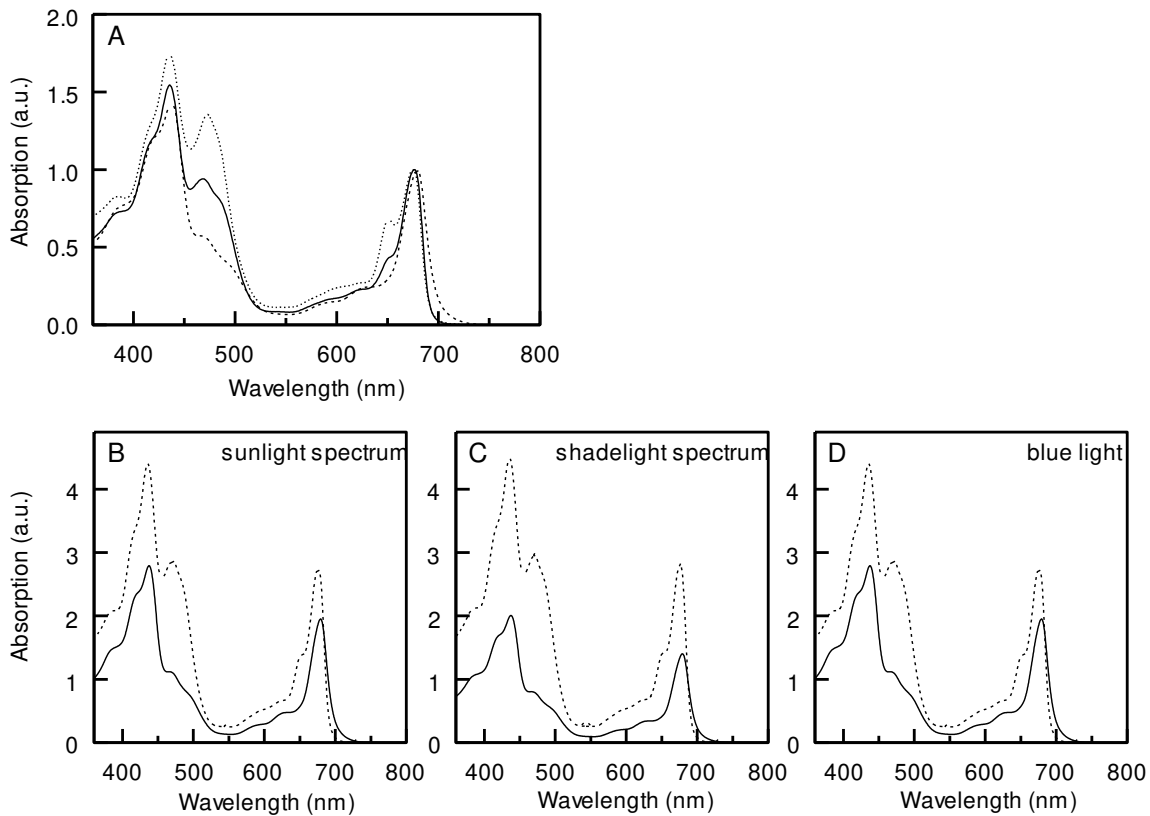


Supplemental Figure 3. Quantification of PSI/PSII ratio by Protein immunoblotting.

(A) Example of one Western blot of thylakoids from leaves grown under a blue light, shadelight and sunlight spectrum. Samples were loaded at four different concentrations and developed with antibodies against CP43 (a PSII core protein) and PsaD (a PSI core protein). Antibodies (Agrisera, Sweden) were diluted 2000x and 7000x for CP43 and PsaD, respectively. The level of antibody binding was monitored with secondary goat anti-rabbit IgG alkaline phosphatase antibody in combination with NBT/BCIP.

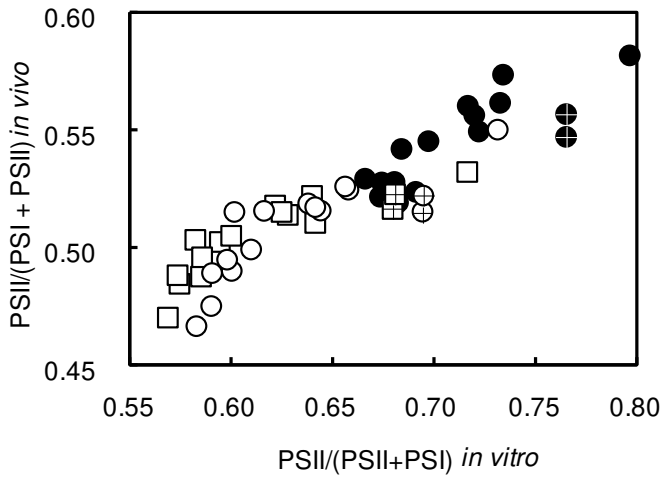
(B) Example of signal linearity verification. Occasionally the last point was out of the linear range due to saturation.

(C) Relative PSI/PSII ratios based on PsaD/CP43 ratios. The ratios for the blue light and shadelight spectrum samples were normalized to the sunlight spectrum sample (set to 1). Error bars represent the s.e.m (N≥5).

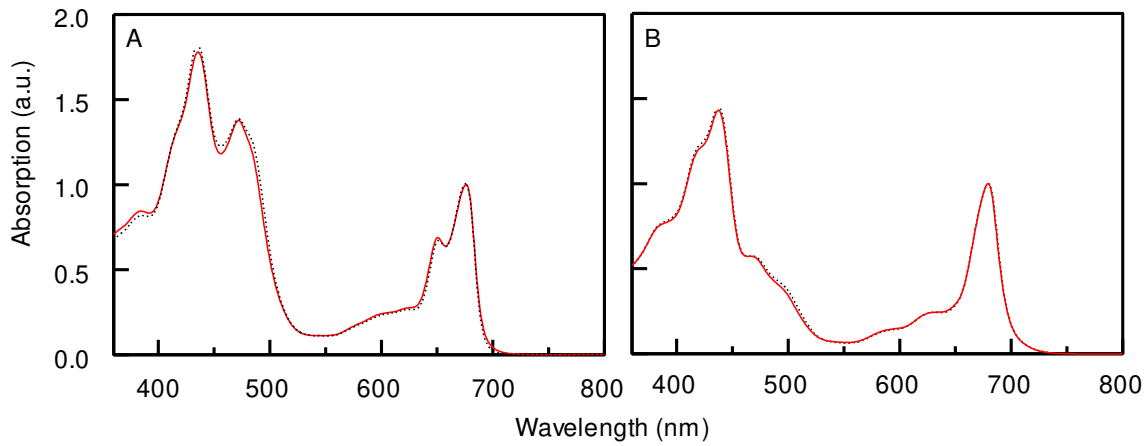


Supplemental Figure 4. (A) Absorbance spectra of LHCII (upper dotted line) and PSI-LHCI (lower dotted line) purified from chloroplasts of the sunlight spectrum grown cucumber leaves (spectra for blue light and shadelight spectrum grown leaves were identical), and that of the PSII C₂S₂M₂ supercomplex of *Arabidopsis thaliana* (connected line). Spectra were normalized to the maximum in the Q_y region. **(B, C, D)** Absorbance spectra of PSI (connected line) and PSII (dotted line) from leaves grown under the three different light spectra, normalized to the number of Chls a and b in each complex, as described in the Methods section of the main text.

Note that at wavelengths >700nm PSII absorbance is close to zero, whereas *in vivo* quantum yields substantially greater than zero were measured at 707 nm and 714 nm (Supplemental Table 2). This is at least partially due to the fact that the narrow-band pass filters used for the *in vivo* measurements (see Methods section of the main text), of which the centre wavelengths are reported, transmitted a small proportion of smaller wavelengths (>690 nm). These smaller wavelengths were partially absorbed by PSII, allowing some linear electron flow and therefore CO₂ fixation.



Supplemental Figure 5. Relationship between the excitation balance of the two photosystems calculated as light fraction absorbed by PSII divided by the absorbed fraction by both PSI and PSII using an *in vitro* and *in vivo* approach (sunlight spectrum: open circles; shadelight spectrum: closed circles; blue light: squares). Only those data points corresponding with wavelengths preferentially exciting PSII are presented in the graph. The six crossed data points correspond with the absorption peaks of carotenoids (460 nm and 500 nm). If these data points are not taken into account, the linearity of the relationship between the *in vitro* and *in vivo* approach improves significantly.



Supplemental Figure 6. Absorbance spectra of the purified LHClI trimer **(A)** and PSI-LHCl **(B)** of sunlight spectrum grown cucumber leaves (red connected lines; spectra for blue light and shadelight spectrum grown leaves were similar), and *Arabidopsis thaliana* (black dotted lines). Due to the negligible differences in the absorbance spectra of the photosystem components of *Cucumis sativus* and *Arabidopsis thaliana* it is difficult to distinguish between the two lines in each graph.

Supplemental Table 1. The wavelength dependence of the quantum yield for CO₂ fixation on an incident light basis ('action spectrum') for *Cucumis sativus* leaves grown under an artificial sunlight spectrum (SUN), an artificial shadelight spectrum (SHADE) and blue light (BLUE). The action spectra are presented on an absolute (i.e. CO₂ molecules fixed per incident photon; left table) and relative basis (right table). Concerning the absolute values (left), the LSD of the significant (P<0.05) interaction between growth-light spectrum and measuring wavelength is 0.0044 (P<0.05). The spectra of the three different growth-light sources are shown in Figure 1 in the print version.

Wavelength (nm)	SUN	SHADE	BLUE
409	0.068	0.065	0.065
427	0.058	0.054	0.058
444	0.058	0.055	0.060
458	0.061	0.056	0.061
477	0.060	0.055	0.062
497	0.062	0.055	0.059
516	0.062	0.058	0.061
539	0.060	0.053	0.060
558	0.057	0.051	0.062
578	0.073	0.062	0.072
599	0.074	0.067	0.078
618	0.081	0.076	0.082
636	0.080	0.078	0.084
657	0.079	0.075	0.083
678	0.080	0.077	0.085
694	0.050	0.052	0.049
707	0.014	0.014	0.012
714	0.008	0.009	0.008
736	0.000	0.000	0.000

Wavelength (nm)	SUN	SHADE	BLUE
409	0.84	0.83	0.77
427	0.72	0.70	0.69
444	0.72	0.71	0.71
458	0.76	0.72	0.72
477	0.74	0.71	0.73
497	0.77	0.72	0.70
516	0.76	0.75	0.72
539	0.75	0.69	0.71
558	0.70	0.66	0.73
578	0.90	0.79	0.85
599	0.92	0.86	0.92
618	1.00	0.98	0.97
636	0.99	1.00	0.99
657	0.98	0.96	0.98
678	0.99	0.99	1.00
694	0.61	0.67	0.58
707	0.17	0.19	0.15
714	0.10	0.11	0.09
736	0.00	0.00	0.00

Supplemental Table 2. The wavelength dependence of the quantum yield for CO₂ fixation on an absorbed light basis for *Cucumis sativus* leaves grown under an artificial sunlight spectrum (SUN), an artificial shadelight spectrum (SHADE) and blue light (BLUE). The quantum yields are presented on an absolute (i.e. CO₂ molecules fixed per absorbed photon; left table) and relative basis (right table). Concerning the absolute quantum yields (left), the LSD of the significant ($P < 0.05$) interaction between growth-light spectrum and measuring wavelength is 0.0059 ($P < 0.05$). The spectra of the three different growth-light sources are shown in Figure 1 in the print version.

Wavelength (nm)	SUN	SHADE	BLUE
409	0.071	0.068	0.068
427	0.061	0.057	0.061
444	0.060	0.058	0.063
458	0.065	0.059	0.064
477	0.063	0.058	0.065
497	0.066	0.059	0.062
516	0.072	0.069	0.069
539	0.082	0.075	0.082
558	0.080	0.074	0.085
578	0.091	0.080	0.091
599	0.089	0.080	0.091
618	0.093	0.089	0.093
636	0.090	0.088	0.093
657	0.085	0.080	0.088
678	0.085	0.082	0.089
694	0.060	0.066	0.058
707	0.024	0.029	0.021
714	0.018	0.022	0.017
736	0.000	0.000	0.000

Wavelength (nm)	SUN	SHADE	BLUE
409	0.77	0.77	0.73
427	0.66	0.64	0.65
444	0.65	0.66	0.67
458	0.70	0.67	0.69
477	0.68	0.65	0.70
497	0.71	0.67	0.67
516	0.77	0.77	0.74
539	0.88	0.85	0.88
558	0.86	0.83	0.91
578	0.98	0.90	0.97
599	0.96	0.90	0.98
618	1.00	1.00	1.00
636	0.97	0.99	1.00
657	0.92	0.90	0.95
678	0.91	0.93	0.96
694	0.64	0.74	0.62
707	0.26	0.32	0.22
714	0.19	0.25	0.18
736	0.00	0.00	0.00